1.

NRL SPECIAL [illegible]JECTS CONTROL NUMBER

NRL B-0037-74

Rec'd 2/21/74

~~TOP SECRET~~ - HANDLE VIA BYEMAN CONTROL SYSTEM

DATE 27JUL73

ORIGINATOR	SERIAL NO.	ENCLOSURES
MITRE CORP.	BYE 18278	-

DATE REC'D	TICKLER DATE	COPY NO.	RECEIPT NO.
2/15/74	-	3	WA 160404

SUBJECT: PROJECT # 8540 (ERROR ANALYSIS FOR SYSTEM 7107 (U)

DIST INFO

DRD 7/6/94

- [ ] BASIC DOCUMENT ON R/S
- [ ] BASIC DOCUMENT NOT HELD. DESTROY.

ROUTE TO	*	CY NO.	W/ ENCL	SIGNATURE	DATE OUT	DATE RETURN
7030		3		R D Mayo	3/3/74	
Tom L				TL		
Dave P.				D & P.		
Loretta				(Ordered 3/12/74 Please order Reference page 35)		

CODES HAVING PRIMARY INTEREST CHECK ONE

- [ ] RETAIN INDEFINITELY. (REFERENCE VALUE).
- [ ] RETAIN ____ MONTHS. (INFO MATERIAL HAVING ONLY TEMPORARY REFERENCE VALUE).
- [ ] DESTROY AFTER ROUTING. (NO FURTHER REFERENCE OR INFORMATION VALUE).

DESTRUCTION REPORT NO.

FINISH FILE

REMARKS

D605

NRL INCOMING DOCUMENT

B037-74

3

BYE-18278-74

7107

Transferred NRO Archives 8-19-05

* A-ACTION
I-INFORMATION
C-COMMENT
R-RETAIN
E-EVALUATION

RETURN THIS ROUTE SLIP TO NRL SPECIAL PROJECTS OFFICE, ROOM 222, BLDG. 43.
DO NOT ROUTE TO OTHER SECTION OR BRANCH.

[AC]TION TAKEN BY

[CON]TROL RECORD NDW-NRL-5216/1005 (REV. 3-72)

12 + 4

MITRE Technical Report

MTR- 6457
No. Vol. Series Rev. Supp. Corr.

CONTROLLED DISTRIBUTION

BYE-18278

Subject: Error Analysis for System 7107 (U)

NSA
PK 044474
2/1/74

Author: J. A. Giordano X2724

Dept.: D-33

Date: 27 July 1973

Project No.: 8540

WA
160404

7030

D605

Department Approval:

and

MITRE Project Approval: Charles W. Sanders

Charles W. Sanders

THE MITRE CORPORATION
893-3500
WASHINGTON, D.C.
OPERATIONS

Page 1 of 57 Pages

COPY 3 OF 7 COPIES

CLASSIFIED by DIRNSA (NSAM 123-2)
EXEMPT FROM GENERAL DECLASSIFICATION
SCHEDULE OF EXECUTIVE ORDER 11652
EXEMPTION CATEGORY 2
DECLASSIFY on Indefinite

NATIONAL SECURITY INFORMATION

Unauthorized disclosure subject to criminal sanction.

HANDLE VIA BYEMAN
CONTROL SYSTEM ONLY

This document was prepared for authorized distribution only.

MCF 1168-1 (U)

NRL B-0037

SECRET EARPOP 1244

ABSTRACT

The accuracy in estimating the Effective Radiated Power (ERP) of emitters from system power measurements and medium loss estimates was investigated. The investigation of system power measurement accuracy considered the calibration tests for the antennas and electronic system, procedures for calibration data retrieval, and variations from calibration test conditions. The resulting error standard deviation ranged from 0.41 db to 0.89 db, depending on radio frequency. The investigation of medium loss estimates considered the accuracy of models for the average medium loss and variations of medium loss with time (fading). Large medium uncertainties resulting from specific medium considerations were identified for low elevation angles and low radio frequencies.

9037-24

TABLE OF CONTENTS

TABLE OF CONTENTS (CONTINUED)

LIST OF ILLUSTRATIONS

LIST OF TABLES

1.0 INTRODUCTION

1.1 Background and Objective

PROJECT ROSTER is a set of analysis activities concerned with the accuracy in estimating the Effective Radiated Power (ERP) of specified emitters from remote power measurements. The particular remote system (7107) being considered in this report makes digital power measurements on intercepted waves for estimating ERP and time of arrival measurements for the purpose of locating emitters by hyperbolic ranging techniques. The accuracy of the ranging procedure known as [redacted] was not investigated. The objective of this task was to determine the accuracy of ERP estimates made from power measurements by the 7107 system. The scope of the investigation reported on herein includes the measurement hardware (payload and antennas), computational procedures, and medium considerations.

1.2 Approach

The ERP estimate is made by use of the following basic equation:

$$ERP = P_r - G + L_M \qquad (1)$$

where

P_r = Power measurement (dbm)

G = Antenna gain (db)

L_M = Medium loss (db)

The P_r and G values are determined from payload and antenna calibration data respectively. Errors in their values result from calibration test inaccuracies and from variations in operational conditions (temperature, frequency, etc.). The net error in the P_r and G values is termed the system power measurement error. The values of L_M are determined from a medium loss model. Errors result in its value due to model inaccuracies in estimating the average loss and due to variations from the average with time (fading). The results from investigating sources of error for both system power measurement and medium loss is reported in section 3.0 and 4.0 respectively of this report.

The approach taken was to identify individual sources (causes) of error and assess their impact on the affected term in equation 1. In order to facilitate the addition of errors in each of the three terms of equation 1, each term was viewed as being subdivided into sums of error perturbed terms in decibel units. Such terms in an error free state corresponded to a unity multiplier. Since errors were independent and added in a random fashion, the net ERP error could be viewed as a random variable which was the sum of random variables. The mean and variance of the ERP error was computed as the sum of the means and variances of individual error terms regardless of their distribution.

2.0 SUMMARY OF RESULTS

The system error in making power measurements on intercepted waves of known polarization is estimated to have a standard deviation ranging from 0.41 db to 0.89 db with increasing radio frequency. This presumes that estimates are made in accordance with the procedures described in this report. (Section 3.6 lists some important processing restrictions.) If it is not known whether the wave is horizontal or vertical, an additional error results which can be computed from equation 2 in this report. Excluding low elevation angles the average medium losses can be estimated without significant additional error, but fading variations due to ionospheric phenomena (scintillations and Faraday fading) will result in an additional highly variable component of error. This fading will diminish with increasing frequency typically disappearing above 1-2 GC. During severe magnetic storms, this fading will result in variations exceeding ±0.5 db eighty-nine percent or more of the time. Generally, however, they will be less severe and even non-existent. The large variability associated with fading allows the possibility of greatly reducing its impact by data selection.

At low elevation angles where the emitter main beam is directed near the horizon (below two degrees) or where significant multipath lobe structure develops in the main beam, additional inaccuracies result. The medium loss model must be modified to consider multipath and diffraction effects. Multipath effects can be removed if the complete emitter antenna pattern is available. The diffraction loss resulting from transmission along the boundary of the earth is much greater than that predicted by a space wave model. A capability to handle low elevation angle data has been implemented on the ADAGE computer and display. It should be pointed out that this capability is limited to low frequencies because the number of power measurements available is inadequate to define the lobe structure at higher frequencies. Experimental testing is necessary to evaluate this capability because of the subjective procedures involved and the medium loss model. A simulation approach could be used to evaluate the procedures performed by the analyst in conjunction with the ADAGE display, if adequate experimental data on medium losses could be acquired to evaluate the medium loss model. In any case, the accuracy of this capability will be less than that of the space wave model. The low elevation angle situation is further deteriorated by additional error caused by tropospheric fading. Its impact will be similar to that of ionospheric fading and it can be combatted by similar procedures.

Methods of reducing the error due to fading fall into two categories: data selection and averaging. Averaging can be used where independent measurements are available to reduce the error in the estimate. Data selection requires that data be judiciously chosen with a minimum of fading present. Data selection can be performed on a short term or long term basis. In the short term case, some quantitative measure (index) of fading activity would be associated with each set of data thus allowing the selection of data with the least fading. A short term probability distribution can be associated with the value of the index to allow evaluation of data accuracy. In the long term case, long term statistics are generated for conditions of interest and used as guidelines for selection and evaluation of data. Guidance in data selection could be provided based on the particular conditions under which the data was taken (i.e., time of day, month of year, elevation angle, etc.). This approach would be used for data in which measures of fading activity are not available. However, consideration must be given in this approach to the possible effects of antenna dependencies. The feasibility of techniques of this type remains an area to be investigated.

3.0 SYSTEM POWER MEASUREMENT ACCURACY

The electronic sensor, consisting of antennas and power measurement instrumentation, intercepts an incoming wave and measures its power at some point in space. The accuracy of the measurement is basically that of the system calibration. This includes the test accuracy of calibration data and the impact of the procedures in which calibration data is used. Since the system is calibrated in two distinct parts, it is appropriate to consider the accuracy of these parts separately. Hence, the analysis of power measurement accuracy divides into two parts: antenna gain accuracy and payload power measurement accuracy.

3.1 Antenna Gain Determination

The system is designed to measure the power of input waves which are vertically, horizontally or circularly polarized with respect to the earth. Antenna gain calibration data is available for both vertically and horizontally polarized input waves. (Antenna gain for a circularly polarized wave can be computed from horizontal and vertical gains.) In order to use the calibration data, antenna pointing angles (ϕ and θ) must be computed by system software. Measurements of the time of arrival of signals at ground stations are used in conjunction with satellite emphemeris data as inputs to system software. Satellite attitude information (pitch, roll and yaw) are optional inputs to the software for correcting altitude variations.

The three basic antenna types are employed over different frequency ranges: monopoles (150-1000 MHz), dipoles (1-10 GC), and horns (above 10 GC). The quarter wave monopoles are mounted around the polar axis of vehicles at various latitudes to provide omnidirectional coverage to vertically and horizontally polarized waves. The half wave dipoles are spaced in quadrature around the equatorial section of vehicles to provide omnidirectional coverage. Dipoles are skewed to provide vertical coverage or when horizontally mounted are combined with additional vertical antennas. High gain horns are also mounted on vehicles.

The calibration data in dipole bands must be combined for several antennas in order to arrive at a composite antenna gain. Each pair of dipoles (spaced by 180 degrees) is calibrated separately and has separate data. In addition, vertical antennas have separate data. The data must be combined in accordance with receiver processing to arrive at the composite antenna gain. In some cases where dipole signals are added, the gains must be added. In other cases (dipoles with vertical antennas), the first output is taken and all others are inhibited for 1024 microseconds. In this case, it is presumed that the largest antenna output power was measured and the largest gain is selected.

The sets of horizontal and vertical calibration data are available for at least one radio frequency in each band. Where multiple frequencies are available a linear interpolation is performed to estimate gain at the desired frequency.

The use of the data also varies with knowledge of the input wave polarization. The following are the four allowable conditions for which the data can be applied:

(1) Input wave known to be horizontal.

(2) Input wave known to be vertical.

(3) Input wave known to be circular.

(4) Input wave known to be either horizontal or vertical.

In the first two cases above, the appropriate horizontal or vertical gain (G_H or G_V) data is selected for use. In the latter two cases, the average gain (equivalently the gain of a linear antenna to circular wave) is used, $G_c = (G_H + G_V)/2$. This results for case (4), in an error which must be added to the system error in a sum of the squares manner. The magnitude of this error is computed as follows:

$$E = \left| \frac{G_H - G_V}{2} \right| \quad (2)$$

3.2 Antenna Gain Calibration Data Accuracy

Antenna pattern and gain calibration tests were performed while antennas were mounted on the vehicle in a tapered anechoic test chamber. Vertically and horizontally polarized waves were emitted from the tapered end of the chamber while the vehicle was oriented in the test region of the chamber. Since, at this short distance, parallax error can occur between the antenna and vehicle coordinate systems, the center of rotation was placed at a point which was judged to be the antenna phase center. The antenna pointing angles (ϕ and θ) and electric field vector orientation angle (τ) are illustrated in Figure 1. The antenna and vehicle axes may be viewed as being the same after being deployed in space. The vehicle vertical axis is stabilized to be perpendicular to the surface of the earth, and thus, goes through the center of the earth. The DP line illustrates the angle of arrival of the incoming wave. As ϕ and θ are rotated, vertically polarized waves remain tangent to lines of longitude, always remaining in the same plane as the vertical axis, and horizontally polarized waves remain tangent to lines of latitude. Any vertical vector on the earth will also intersect the vehicle axis at the center of the earth. Thus, ensuring that it will also be in the same plane.

The test setup for pattern measurements is illustrated in Figure 2. The field in the chamber is maintained constant while measurements of received power levels are made. Output power measurements are printed out to the nearest decibel at five degree increments of ϕ and θ (3D data). In addition, an analog pattern over ϕ was taken for θ equal to 120 degrees (2D data). Antenna gains were measured at a reference point of the pattern by the substitution method. The test antenna was replaced by a standard antenna and the difference in gain between the two antennas observed on a sensitive watt meter.

The investigation of errors in pattern measurements begins with the investigation of the constant input field. Any variations in the magnitude of the input field in the chamber volume will result in

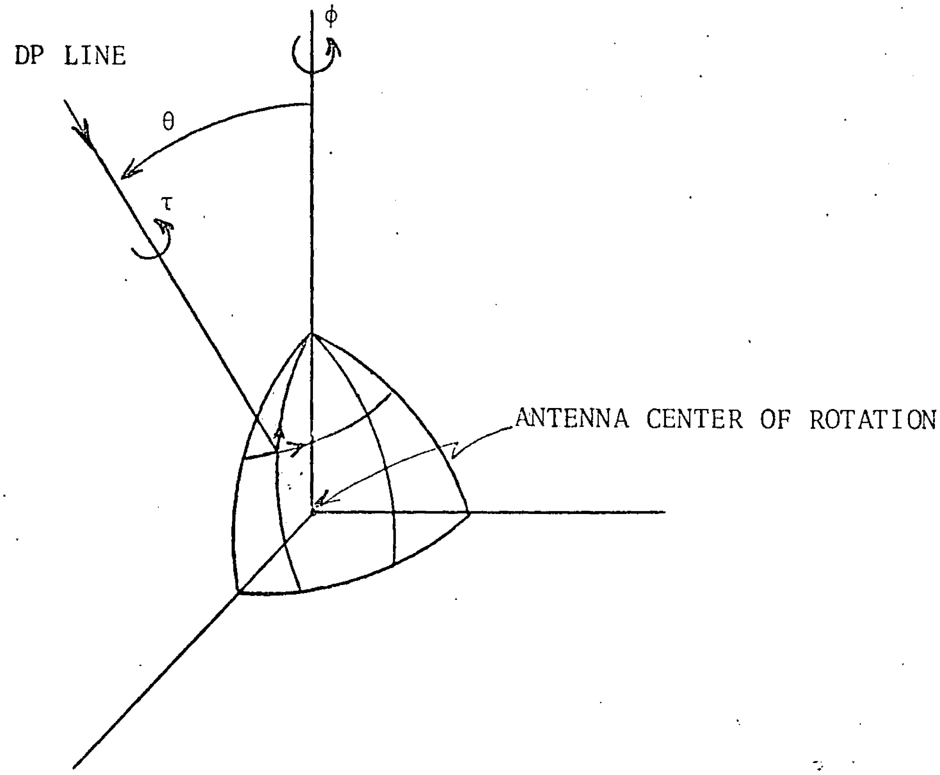

FIGURE 1

ANTENNA COORDINATE SYSTEM

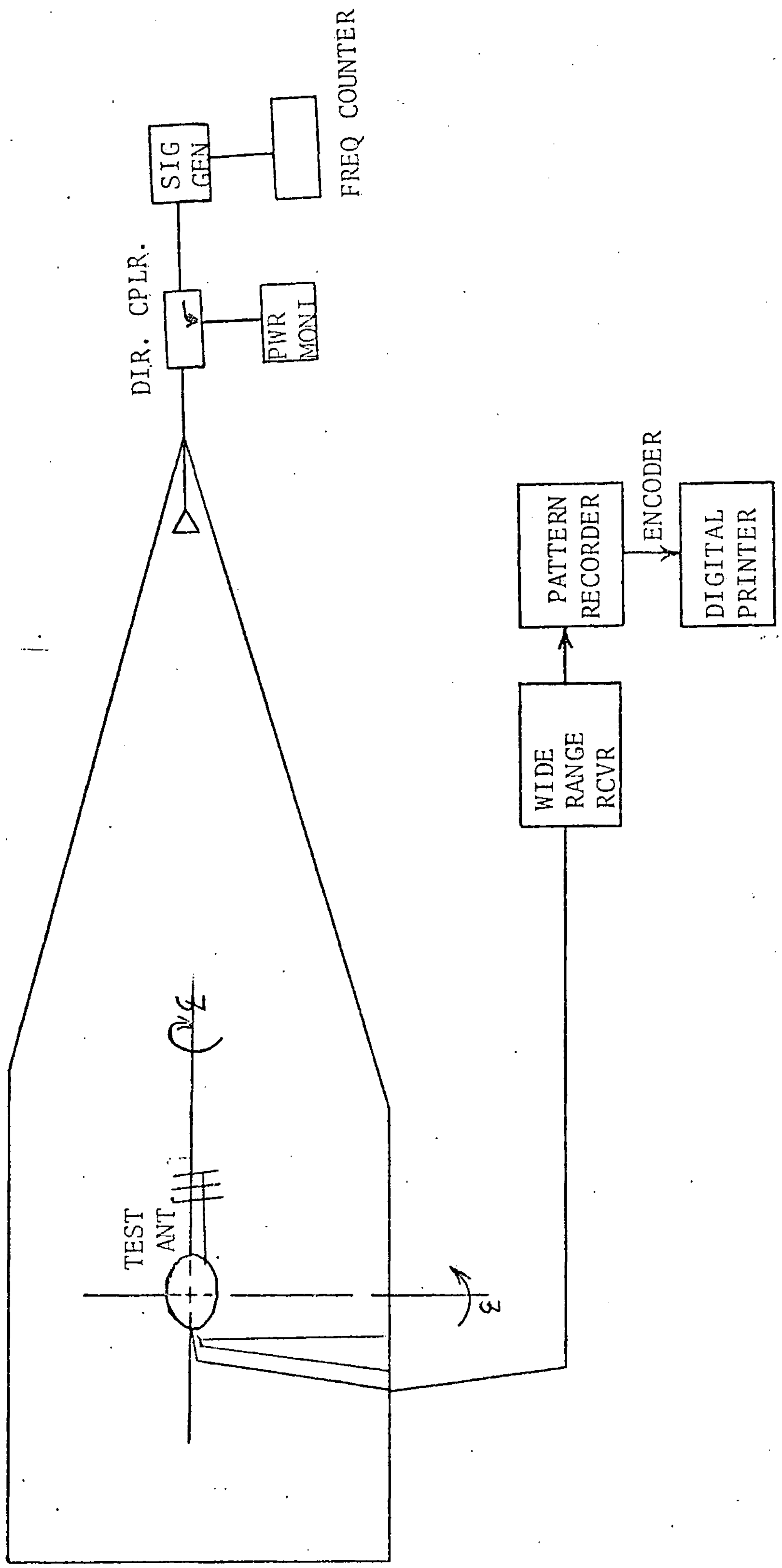

FIGURE 2

TEST CONFIGURATION FOR PATTERN MEASUREMENTS pattern error. Data on volume variations due to chamber reflections was available from the chamber acceptance report.(1) The report also provided computed values of the maximum pattern error. This information is presented in Table I.

TABLE I

MAXIMUM PATTERN ERROR (DB) VS. FREQUENCY

Frequency	Antenna Pattern Levels (Relative to Main Beam)				
	0 db	-10 db	-20 db	-30 db	-40 db
120 MHz	0.2	0.55	1.7	8.0	α
400 MHz	0.1	0.35	1.1	4.0	α
3.0 GHz	<0.1	<0.1	0.15	0.5	1.5
10.0 GHz	<0.1	<0.1	<0.1	<0.1	0.25

All errors are assumed to be uniformly distributed between plus and minus maximum. It is assumed that pattern levels below -20 db are not used. The average variance for the three uniformly distributed errors (0, -10, and -20 db pattern levels) has been computed for each frequency. The results are presented in Table II.

TABLE II

PATTERN ERROR VARIANCE AT DIFFERENT FREQUENCIES

Frequency	Variance
120 MHz	0.36
400 MHz	0.16
3.0 GHz	0.00
10.0 GHz	0.00

Another source of test error is associated with power measurements at the antenna output. The accuracy of the actual power measurements is different from the power meter accuracy because both the pattern measurements and the gain measurements (by the substitution method) are really only differences in scale readings and not absolute power measurements. Other factors entering into measurement accuracy are meter mismatch and reading accuracy. However, since pattern measurements were rounded off to the nearest decibel, a large error uniformly distributed between ±0.5 db and -0.5 db resulted. As long as the measurement error is not significantly larger than this error, this figure should be a good approximation for the net measurement error. An error variance of 0.083 was computed for a uniform distribution. The accuracy will be slightly better when the 2D data is used, but a separate figure was not determined.

3.3 Frequency Interpolation Error

An additional source of antenna gain error is related to the usage of data at specific frequencies. Since data is only available at discrete frequencies, interpolation is performed to determine values of gain at interim frequencies. Interpolation error will depend on the gain difference existing between two frequencies being interpolated between. In order to investigate gain differences, data samples were taken for bands having two or three calibration frequencies. This data is presented in Appendix I. A summary of computed average gain differences for different frequency ranges is presented in Table III.

The standard deviation for linear interpolation error was estimated to be ten percent of the gain difference.

TABLE III

FREQUENCY INTERPOLATION ERROR

Frequency Range (MC)	Average Gain Difference (db)	Estimated Variance
Below 200	5.2	0.27
200-1000	3.5	0.12
Above 1000	0.9	0.01

3.4 Antenna Pointing Angle Accuracy

A final source of antenna gain error is due to the possible inaccuracy of antenna pointing angles. Since the error in test chamber angle measurement is less than 0.1 of a degree, it is not a factor to be considered. The inaccuracy to be investigated concerns the computation of pointing angles by system software from the location of the emitter and satellite. The location of the emitter is computed from time of arrival data and satellite emphemeris data. Emitter location error information is available in the form of a two dimensional error ellipse from system software. The error in satellite location is considerably less than that of emitter location (less than 0.5 nautical miles) and hence, need not be considered.

3.4.1 Impact of Vehicle Orientation Error on Antenna Pointing Angles

The computation of pointing angles is also affected by the vehicle orientation (pitch, yaw, and roll). The vehicle is maintained at a fixed attitude, but variations in this orientation do occur. The magnitude of such variations are computed from payload sensor data and hence can be used to correct the assumed orientation. (The system software has provision for this input.) If this option is not utilized, such errors can not only result in pointing angle errors, but also errors in the tilt of the incoming wave. A review of samples of variations in orientation indicated maximum errors to be approximately as follows:

Pitch = ±3 degrees

Yaw = ±3 degrees

Roll = ±1.5 degrees

The impact, from geometric considerations, of pitch, roll, and yaw error is given in matrix form in equation 3.

$$\begin{vmatrix} \Delta\phi \\ \Delta\theta \\ \Delta\tau \end{vmatrix} = \begin{vmatrix} \pm\ (0\text{-}0.5) & \pm\ (0\text{-}0.5) & \pm\ (1.00) \\ \pm\ (0\text{-}1.0) & \pm\ (0\text{-}1.0) & \pm\ (0.0) \\ \pm\ (1.0) & \pm\ (1.0) & \pm\ (0.0) \end{vmatrix} \begin{vmatrix} \Delta P \\ \Delta R \\ \Delta Y \end{vmatrix} \quad (3)$$

The matrix relates pitch, roll, and yaw variations (ΔP, ΔR, and ΔY, respectively) to resulting antenna pointing angle variations ($\Delta\phi$ and $\Delta\theta$) and tilt angle variation ($\Delta\tau$). The transitional matrix relates the range of impact of individual input parameter variations on individual output parameters. These ranges were determined by a geometric model as illustrated in Figure 3. For example, for a vector at the particular